When is a trend meaningful? Insights to carbon cycle variability from an initial-condition large ensemble

Gordon B. Bonan[1], Clara Deser[1], William R. Wieder[1,2], Danica L. Lombardozzi[3,1], and Flavio Lehner[4,1,5]

[1] Climate and Global Dynamics Laboratory, NSF National Center for Atmospheric Research, Boulder, CO, USA

[2] Institute of Arctic and Alpine Research, University of Colorado Boulder, Boulder, CO, USA

[3] Department of Ecosystem Science & Sustainability, Colorado State University, Fort Collins, CO, USA

[4] Department of Earth and Atmospheric Sciences, Cornell University, Ithaca, NY, USA

[5] Polar Bears International, Bozeman, MT, USA

Supplementary Information

This file contains Supplementary Tables 1–3 and Supplementary Figures 1–11

Supplementary Table 1. Annual gross primary production (g C m^{-2} yr^{-1}) for Harvard Forest. Data for Urbanski et al. (2007) (ref. 13) are for 28 October of the preceding year to 27 October of the nominal year. Data for Finzi et al. (2020) (ref. 19) are for 1 November–31 October. Data for Munger (2022) (ref. 56) are the GPP_NT_VUT_REF product.

Year	Urbanski et al. (2007)	Finzi et al. (2020)	Munger (2022)
1992	1180	1176	1144.71
1993	1350	1354	1304.13
1994	1230	1233	1300.54
1995	1260	1260	1288.33
1996	1330	1328	1363.77
1997	1400	1401	1408.80
1998	1210	1207	1224.14
1999	1400	1405	1341.12
2000	1450	1451	1473.35
2001	1630	1629	1627.03
2002	1520	1523	1589.89
2003	1530	1525	1498.36
2004	1710	1711	1742.67
2005		1387	1430.29
2006		1638	1667.37
2007		1636	1599.17
2008		1602	1590.79
2009		1791	1886.52
2010		2133	1981.20
2011		1885	1713.37
2012		1679	1778.40
2013		1496	1498.92
2014		1562	1704.41
2015		1605	1900.64
2016			1614.45
2017			1436.06
2018			1547.58
2019			1520.98
2020			1262.28

Supplementary Table 2. Annual gross primary production (g C m^{-2} yr^{-1}) for Morgan-Monroe State Forest. Data are the GPP_DT_VUT_REF product (ref. 57).

Year	Novick and Phillips (2022)
1999	1475.59
2000	1558.25
2001	1672.48
2002	1792.80
2003	1657.35
2004	1628.47
2005	1777.55
2006	1670.40
2007	1765.63
2008	1706.37
2009	1527.43
2010	1689.31
2011	1503.34
2012	1482.62
2013	1742.91
2014	1728.41
2015	1645.15
2016	1824.30
2017	1624.98
2018	1768.49
2019	1804.86
2020	1630.84

Supplementary Table 3. Annual gross primary production (g C m^{-2} yr^{-1}) for Howland Forest (ref. 20).

Year	Hollinger et al. (2021)
1996	1309.55
1997	1371.29
1998	1417.03
1999	1395.44
2000	1510.84
2001	1534.20
2002	1332.09
2003	1228.88
2004	1342.55
2005	1286.68
2006	1315.27
2007	1236.06
2008	1296.15
2010	1373.66
2011	1354.56
2012	1357.47
2013	1289.95
2014	1158.15
2015	1280.07
2016	1270.82
2017	1246.96
2018	1317.60
2019	1306.30
2020	1267.00

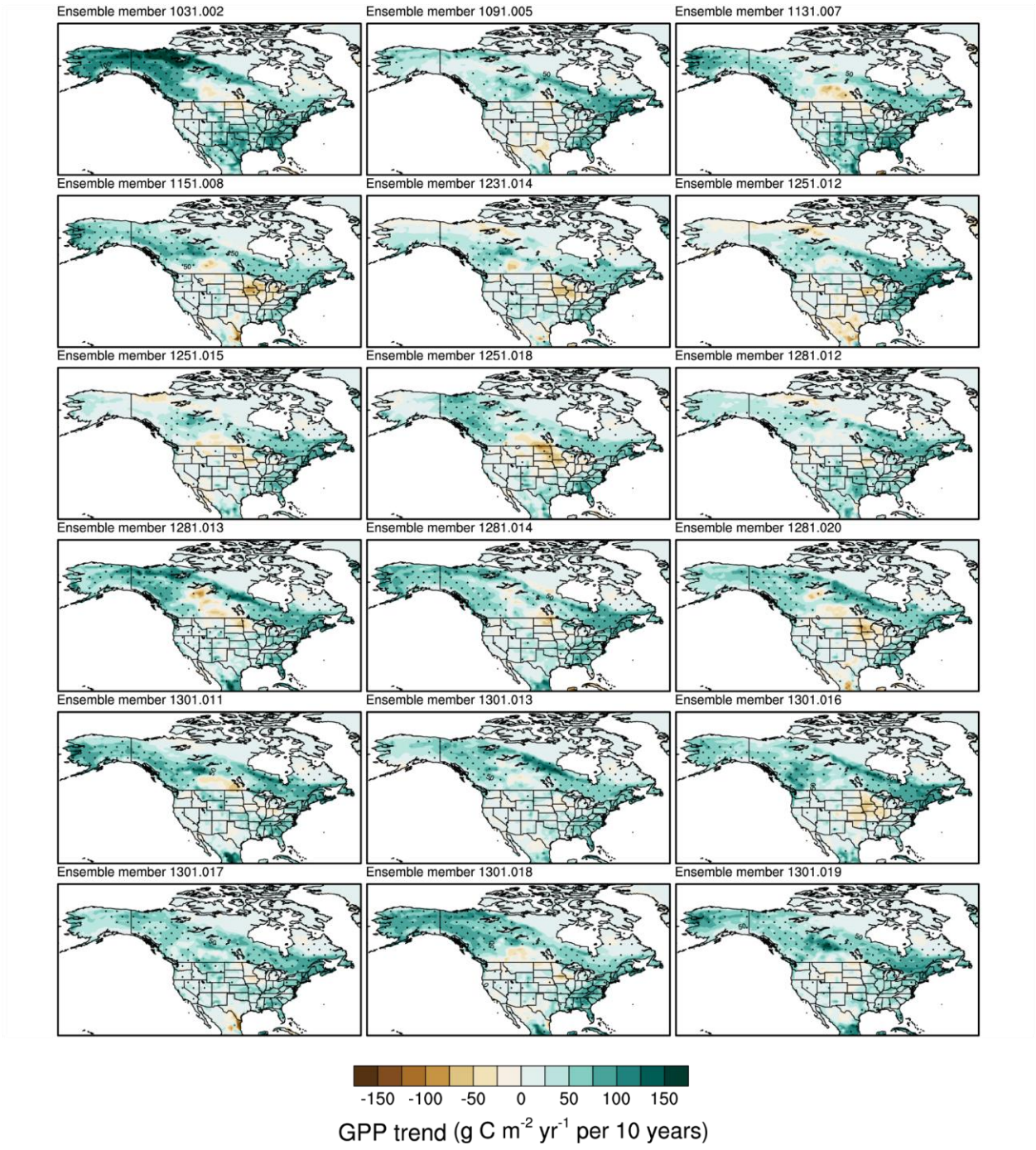

Supplementary Fig. 1. Trends in annual GPP for 1991–2020 in 18 randomly chosen ensemble members. Stippling denotes statistical significance (*n* = 30 years; $p \leq 0.05$).

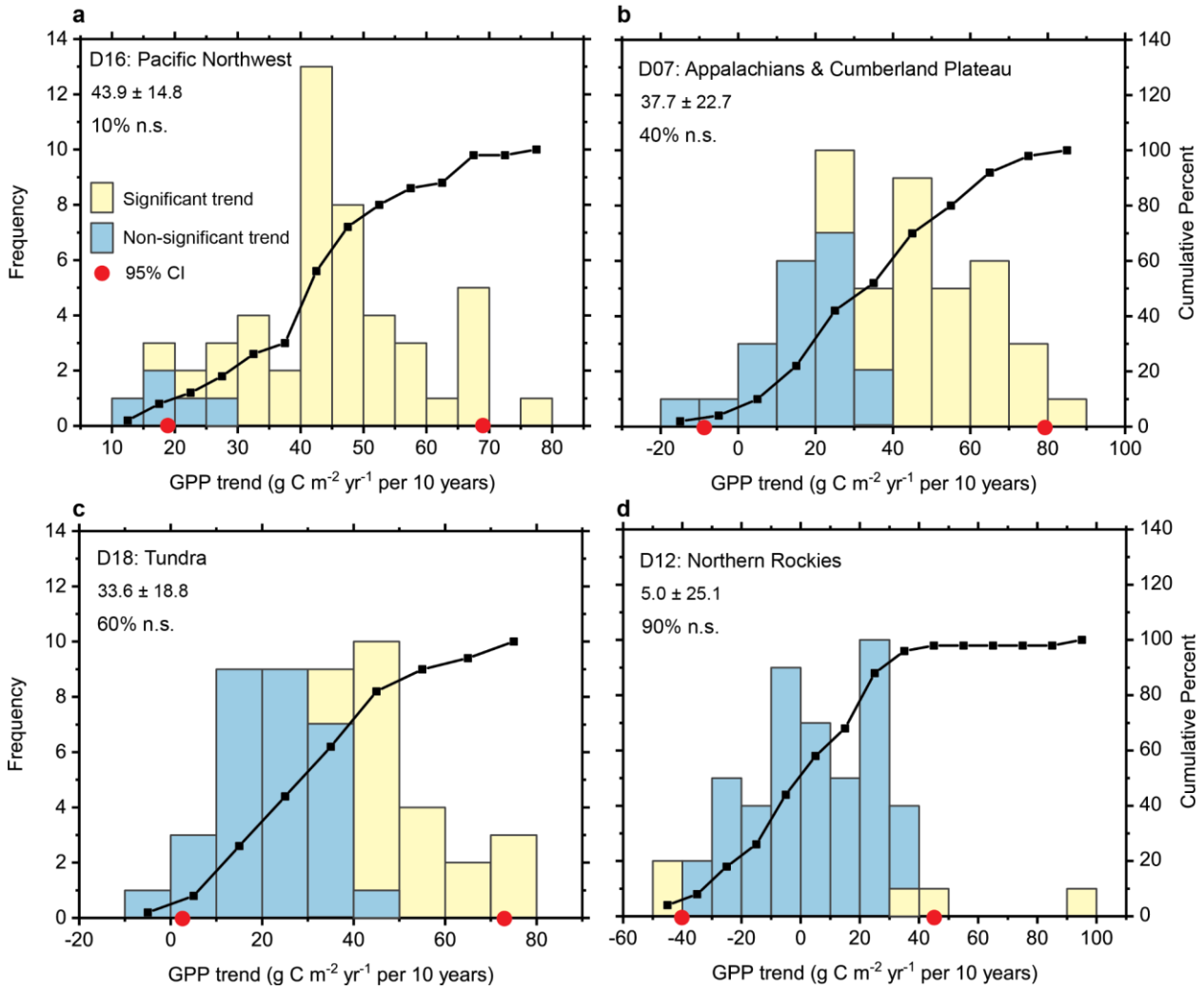

Supplementary Fig. 2. Histogram of annual GPP trends for 1991–2020 at four grid cells. Grid cells correspond to the location of core terrestrial sites for four domains in the National Ecological Observatory Network (NEON). See Fig. 1 for the location of the sites. Panels show (**a**) D16: Pacific Northwest, (**b**) D07: Appalachians & Cumberland Plateau, (**c**) D18: Tundra, and (**d**) D12: Northern Rockies sites. The left axis is the frequency distribution for the n = 50 ensemble members, and the black line is the cumulative distribution (right axis). Yellow shading shows members with a statistically significant trend (n = 30 years; $p \leq 0.05$), and light blue shading shows non-significant trends. The mean ± standard deviation and the percentage of members with a non-significant (n.s.) trend are provided in the upper left of each panel. Also shown is the 95% confidence interval (red circles) obtained as the range of trends (n = 48) after excluding the smallest and largest trends.

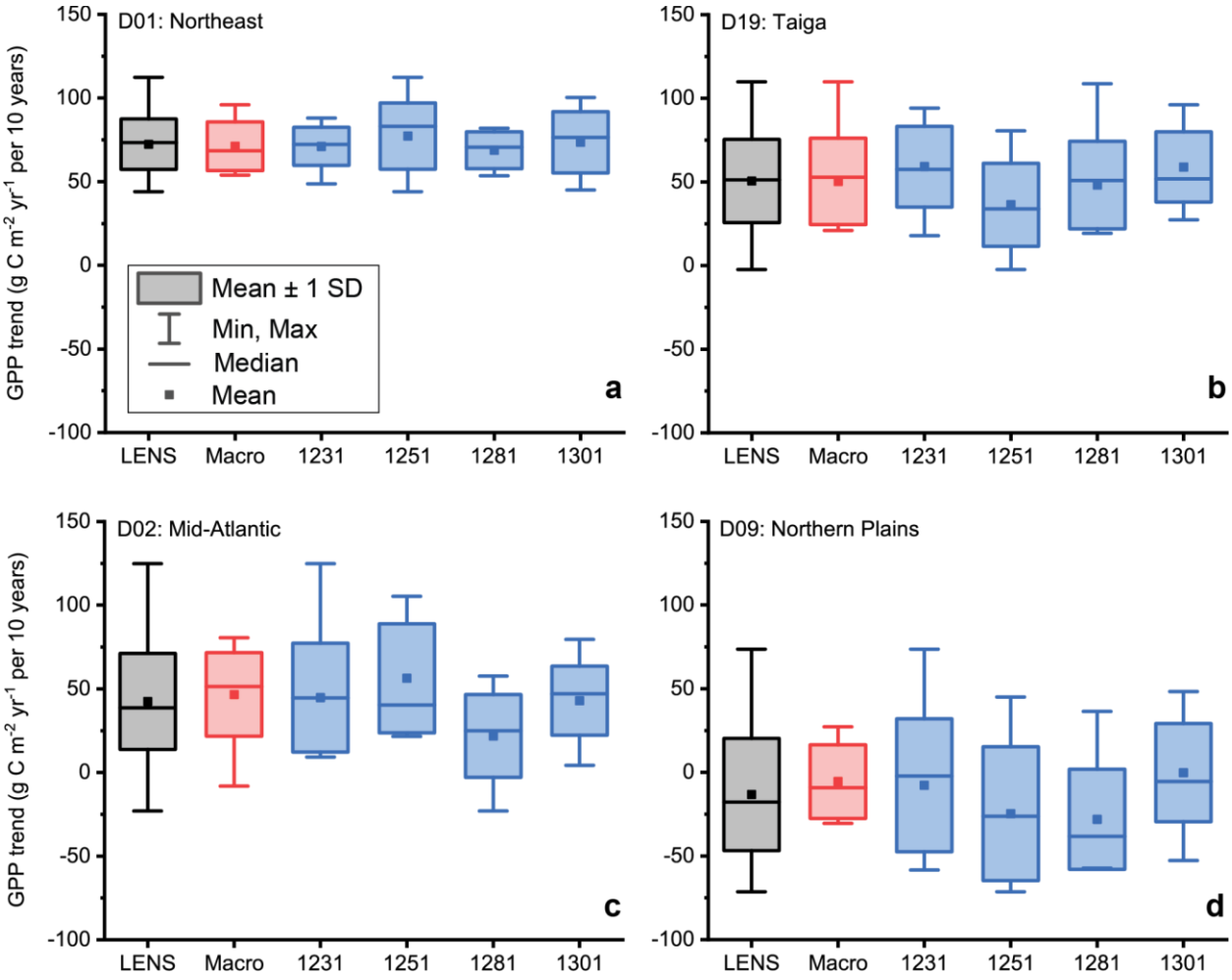

Supplementary Fig. 3. Box plots of annual GPP trends for 1991–2020. Trends are given for the full 50-member large ensemble (LENS), the 10-member macro-initialization (Macro), and the four sets of micro-initializations with 10-members each (start years 1231, 1251, 1281, and 1301 of the preindustrial control). The 10-member macro-initialization simulations differ in start year. The 10-member micro-initialization simulations have the same start year and differ only in a 10^{-14} K perturbation to initial air temperature. Four different start years are used for a total of 40 micro-initialization simulations. Plotted are the mean ± one standard deviation, the minimum and maximum, and the median. Trends are shown for the grid cells corresponding to NEON core terrestrial sites for (**a**) D01: Northeast, (**b**) D19: Taiga, (**c**) D02: Mid-Atlantic, and (**d**) D09: Northern Plains. These are the four grid cells in Fig. 2.

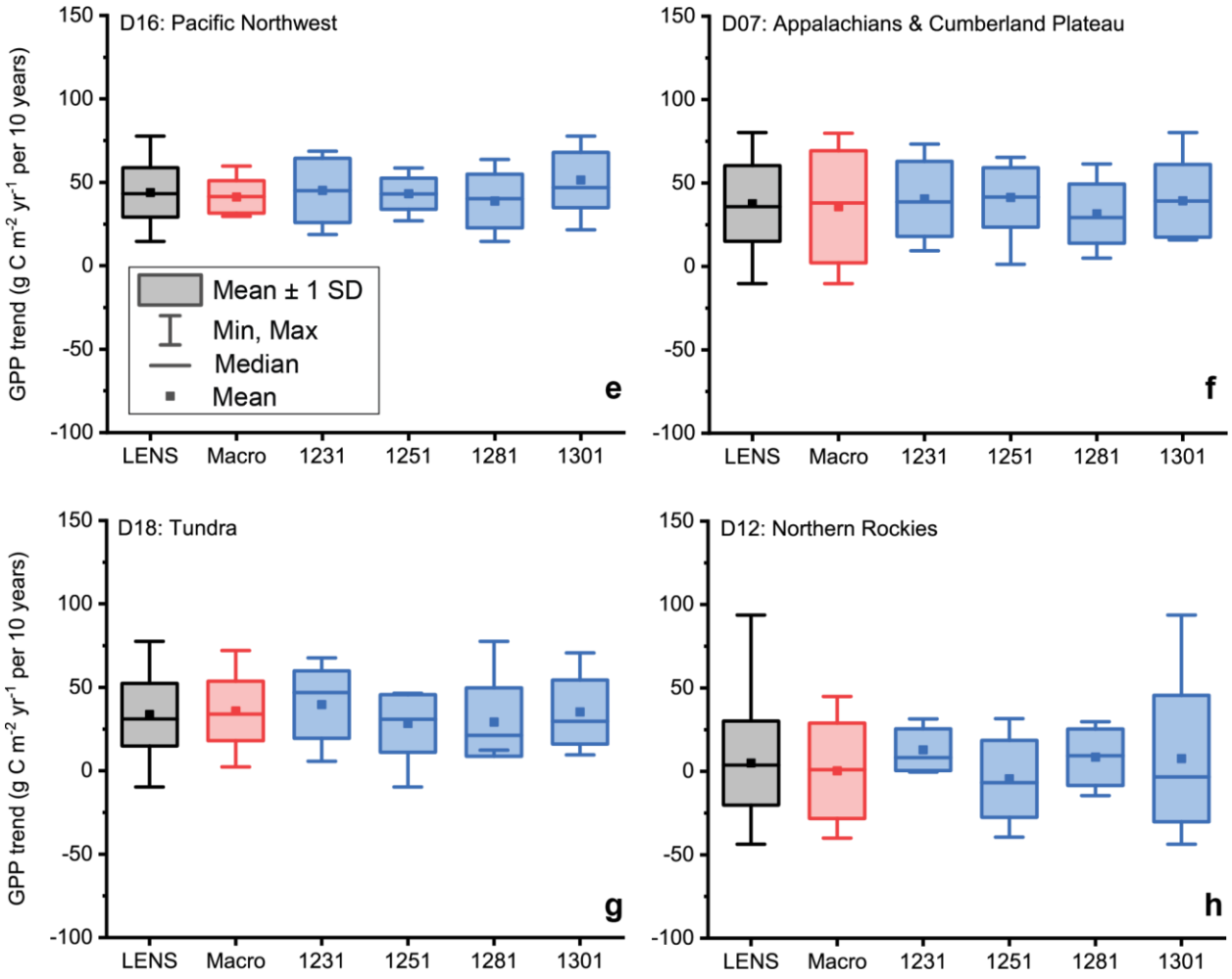

Supplementary Fig. 3 (continued). (**e**) D16: Pacific Northwest. (**f**) D07: Appalachians & Cumberland Plateau. (**g**) D18: Tundra. (**h**) D12: Northern Rockies. These are the four grid cells in Supplementary Fig. 2.

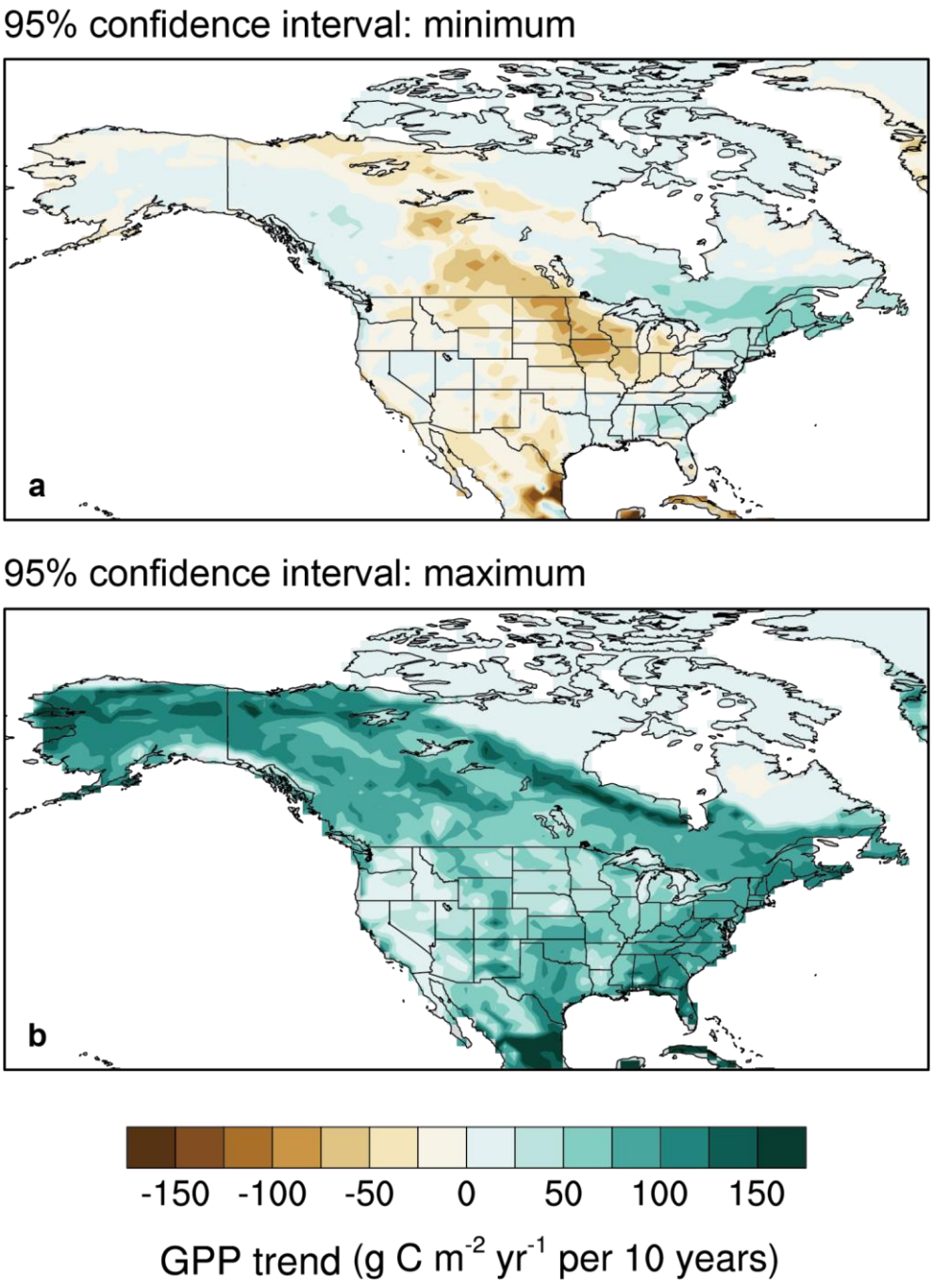

Supplementary Fig. 4. 95% confidence interval in annual GPP trends for 1991–2020. Shown are the (**a**) low and (**b**) high values for the 95% confidence interval obtained from the 50-member ensemble. These are the trends after excluding the smallest and largest trends for each grid cell.

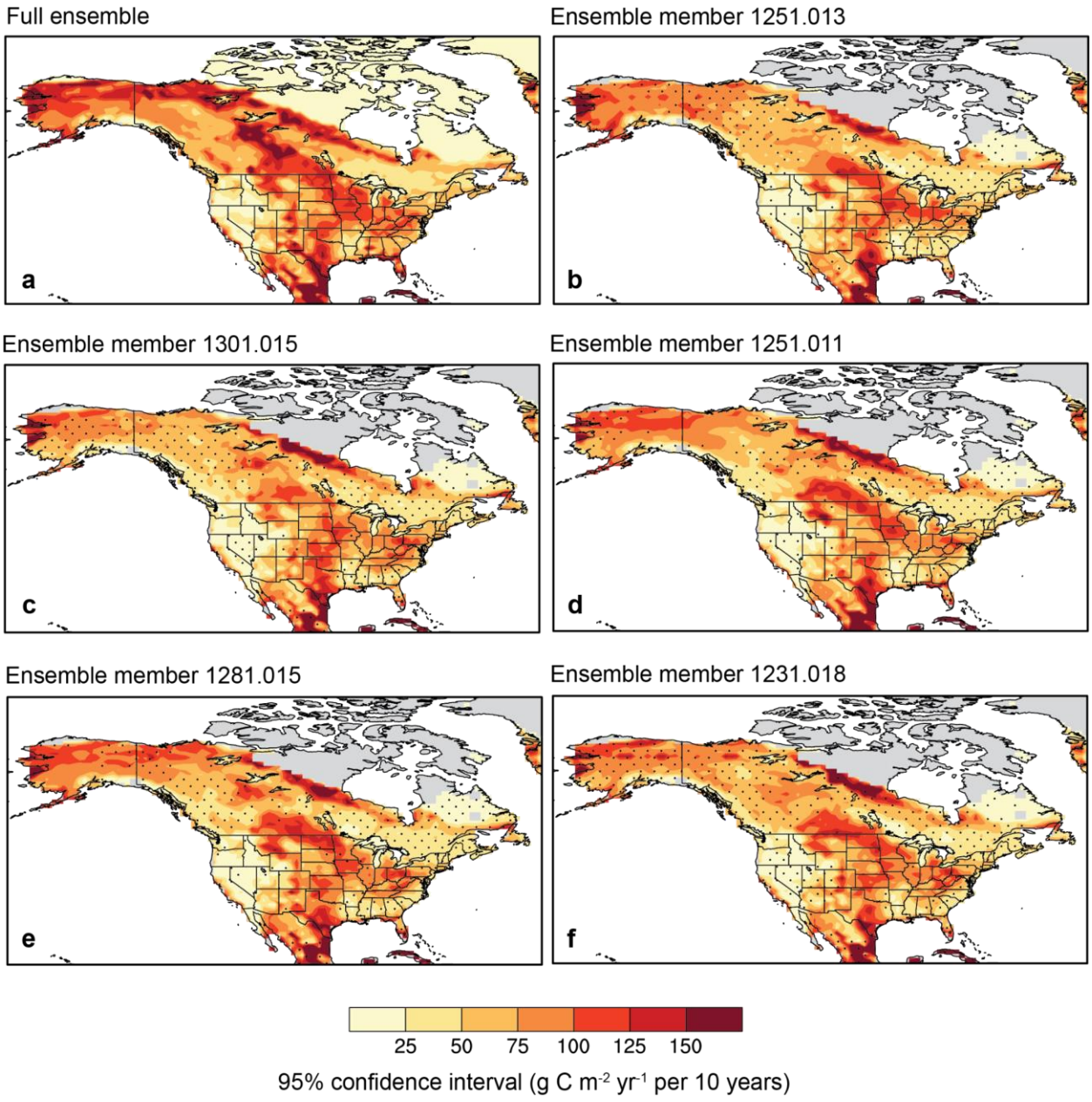

Supplementary Fig. 5. 95% confidence interval in annual GPP trends for 1991–2020. In (**a**), the 95% confidence interval is obtained from the 50-member ensemble. It is the range of trends (*n* = 48) after excluding the smallest and largest trends for each grid cell. Panels (**b–f**) show the 95% confidence interval obtained from the standard error of the regression trend (s_{b1}, equation 3). The confidence interval is $2 * 2.048 * s_{b1}$, where $t_{0.975,28} = 2.048$ is the critical t-value for $n = 30$ years of data. Shown are (**b–d**) three ensemble members chosen at random, (**e**) the ensemble member in Fig. 1c, and (**f**) the ensemble member in Fig. 1d. Stippling shows where the trend is statistically significant (*n* = 30 years; $p \leq 0.05$) for the particular ensemble member.

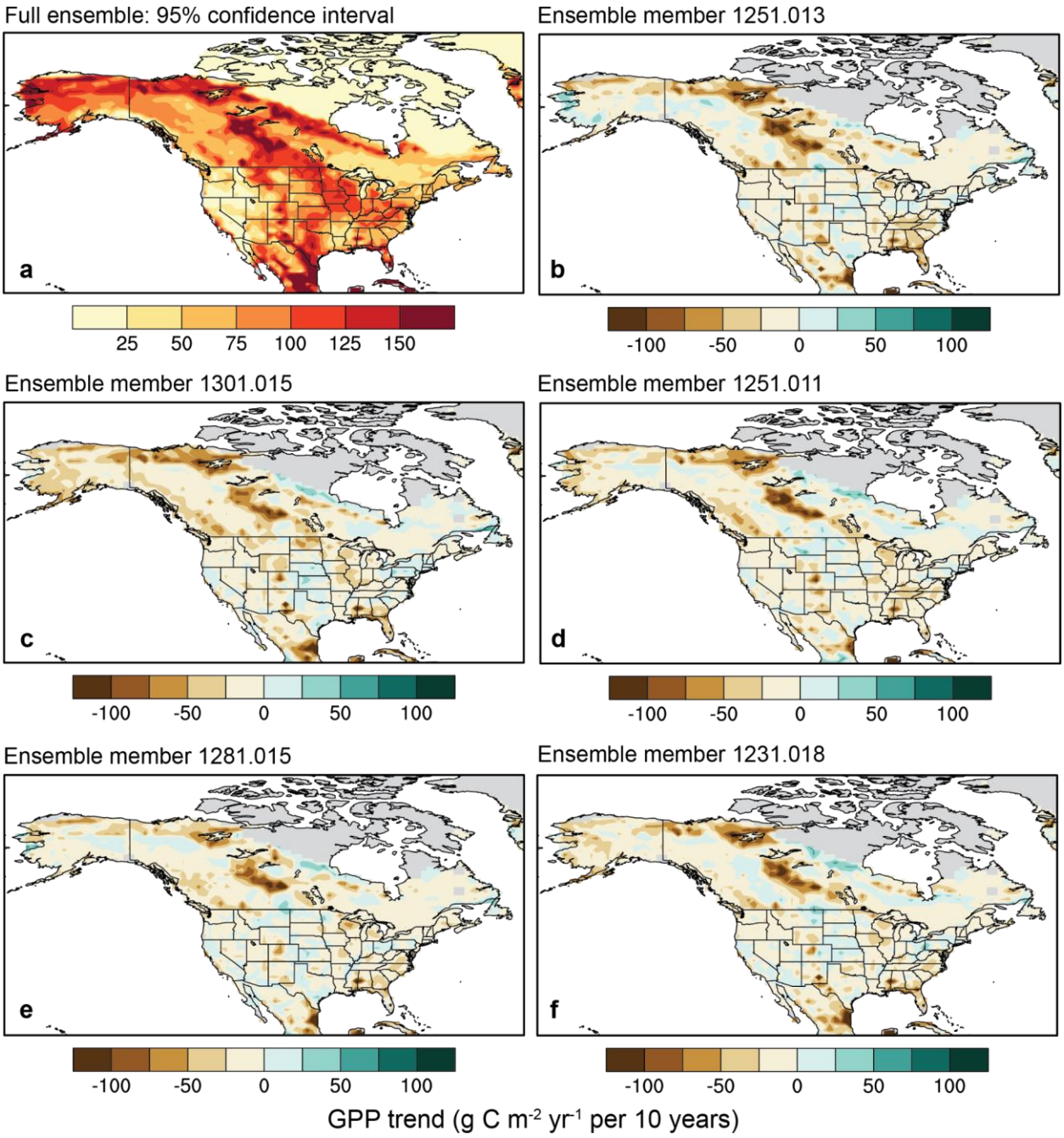

Supplementary Fig. 6. 95% confidence interval in annual GPP trends for 1991–2020. In (**a**), the 95% confidence interval is obtained from the 50-member ensemble. It is the same as Supplementary Fig. 5a. Panels (**b–f**) are as in Supplementary Fig. 5, but show the difference from (**a**).

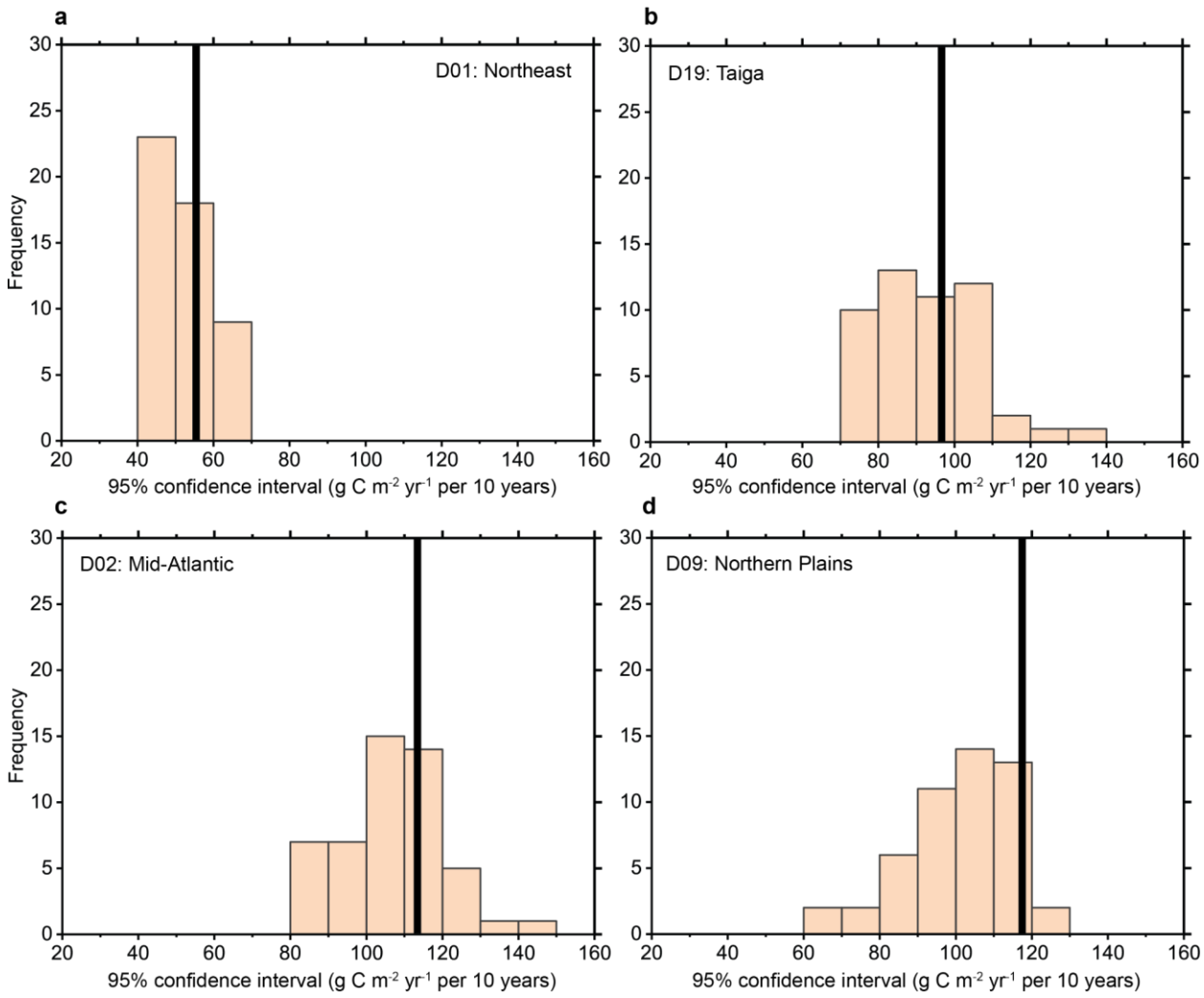

Supplementary Fig. 7. 95% confidence interval in annual GPP trends for 1991–2020 at individual grid cells. The 95% confidence interval obtained from the standard error of the regression trend for each of the 50 ensemble members is shown as a histogram. The confidence interval is $2 * 2.048 * s_{b1}$, where s_{b1} is the standard error of the trend (equation 3) and $t_{0.975,28} = 2.048$ is the critical t-value for $n = 30$ years of data. The thick black line is the 95% confidence interval obtained from the 50-member ensemble. It is the range of trends (*n* = 48) after excluding the smallest and largest trends for each grid cell. Confidence intervals are shown for the grid cells corresponding to NEON core terrestrial sites for (**a**) D01: Northeast, (**b**) D19: Taiga, (**c**) D02: Mid-Atlantic, and (**d**) D09: Northern Plains. These are the four grid cells in Fig. 2.

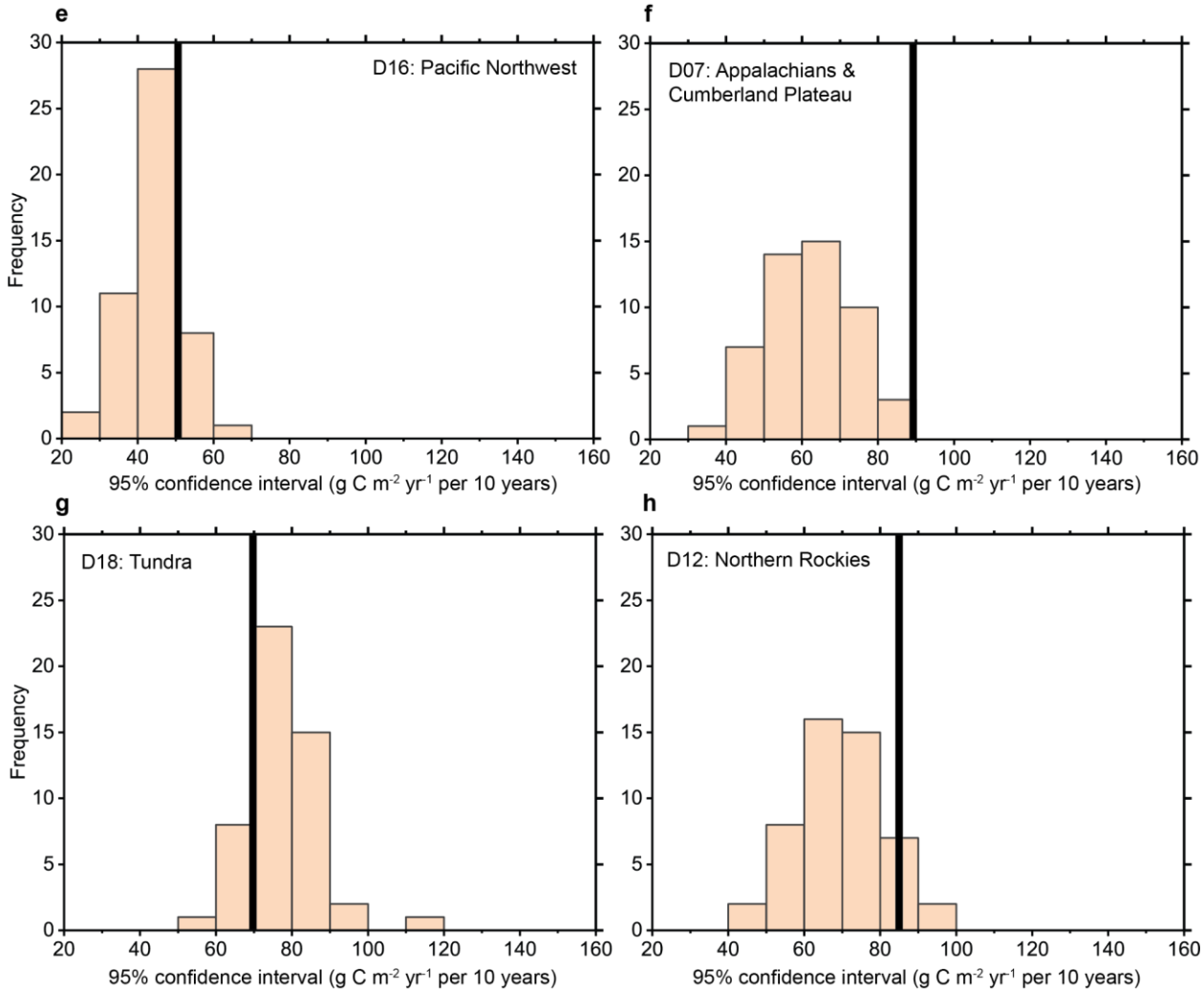

Supplementary Fig. 7 (continued). (**e**) D16: Pacific Northwest. (**f**) D07: Appalachians & Cumberland Plateau. (**g**) D18: Tundra. (**h**) D12: Northern Rockies. These are the four grid cells in Supplementary Fig. 2.

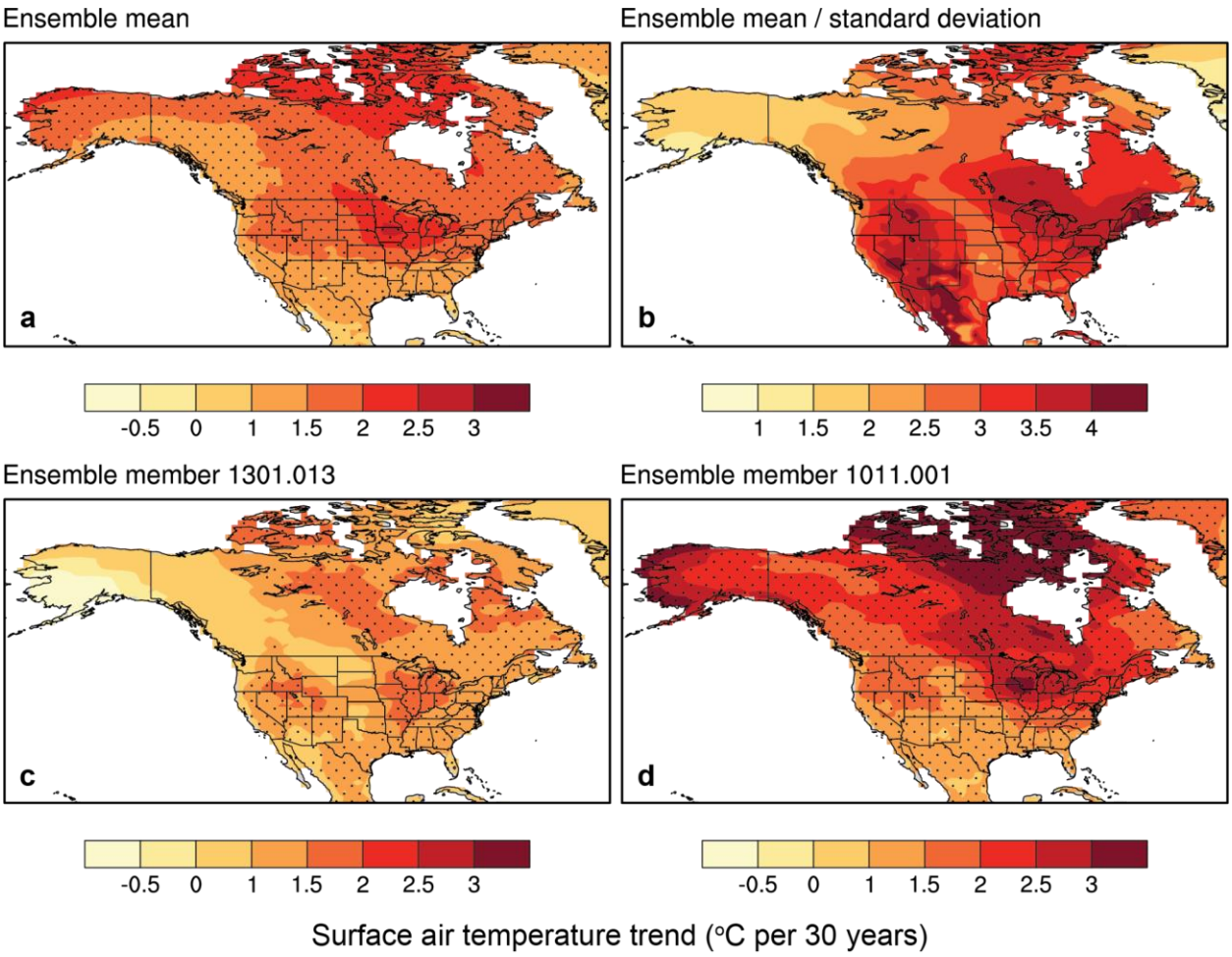

Supplementary Fig. 8. Trends in annual mean surface air temperature (TSA) for 1991–2020. (**a**) Mean trend for the 50-member ensemble obtained from the ensemble mean time series. (**b**) Signal-to-noise ratio defined as the ensemble mean trend (absolute value) divided by the standard deviation of trends across the 50 members. Also shown are trends for two members with small (**c**) and large (**d**) continental mean trends. Ensemble members 1301.013 and 1011.001 are the members at the 3rd (6th percentile) and the 47th (94th percentile) ranks, respectively, based on continental mean trends. Stippling denotes statistical significance (n = 30 years; $p \leq 0.05$) using the ensemble mean time series or the individual ensemble member time series. Trends are multiplied by 30 to report the change in temperature over the 30-year period.

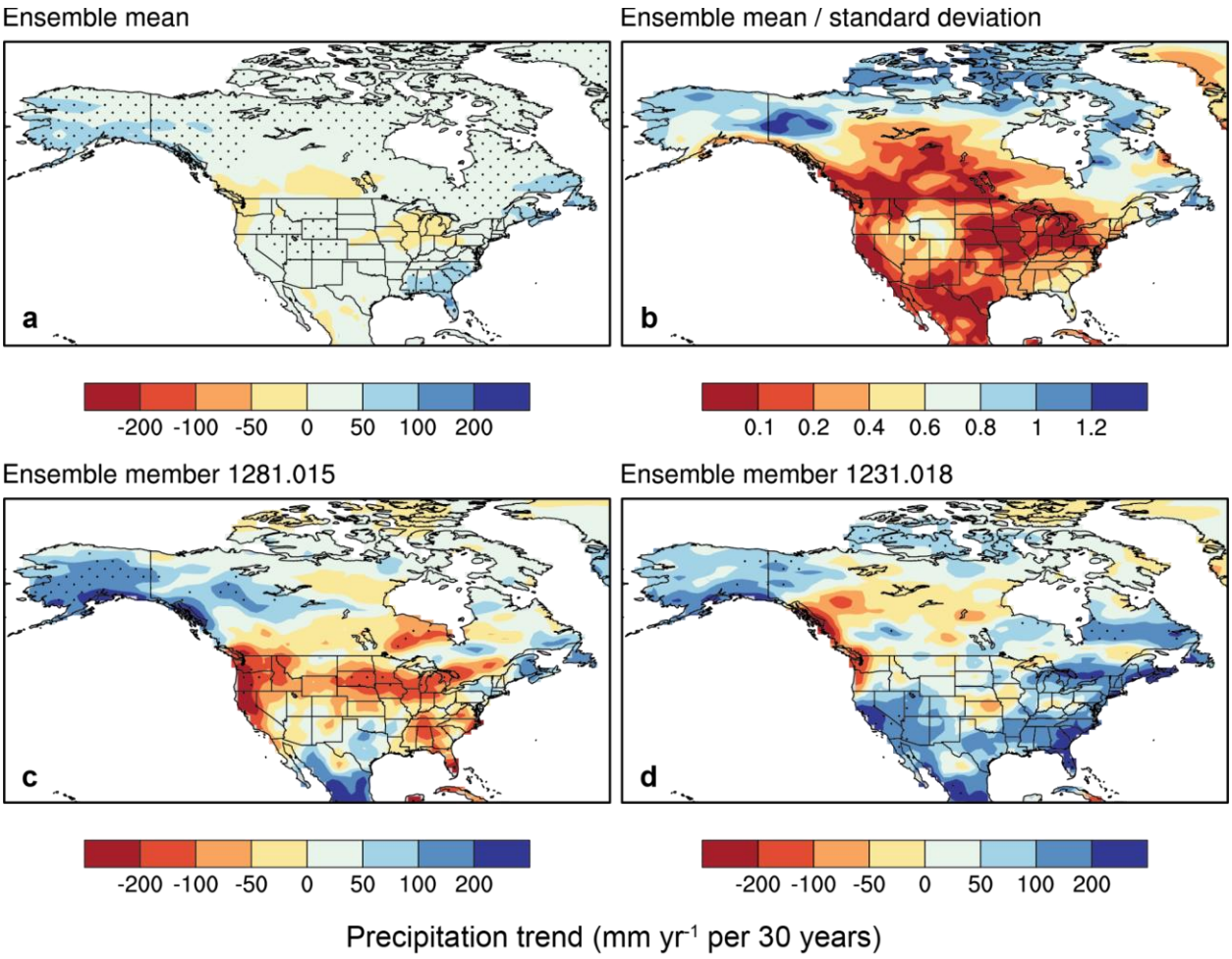

Supplementary Fig. 9. Trends in annual precipitation for 1991–2020. (**a**) Mean trend for the 50-member ensemble obtained from the ensemble mean time series. (**b**) Signal-to-noise ratio defined as the ensemble mean trend (absolute value) divided by the standard deviation of trends across the 50 members. Also shown are trends for two members with small (**c**) and large (**d**) continental mean trends. Ensemble members 1281.015 and 1231.018 are the members at the 3rd (6th percentile) and the 47th (94th percentile) ranks, respectively, based on continental mean trends. Stippling denotes statistical significance (n = 30 years; $p \leq 0.05$) using the ensemble mean time series or the individual ensemble member time series. Trends are multiplied by 30 to report the change in precipitation over the 30-year period.

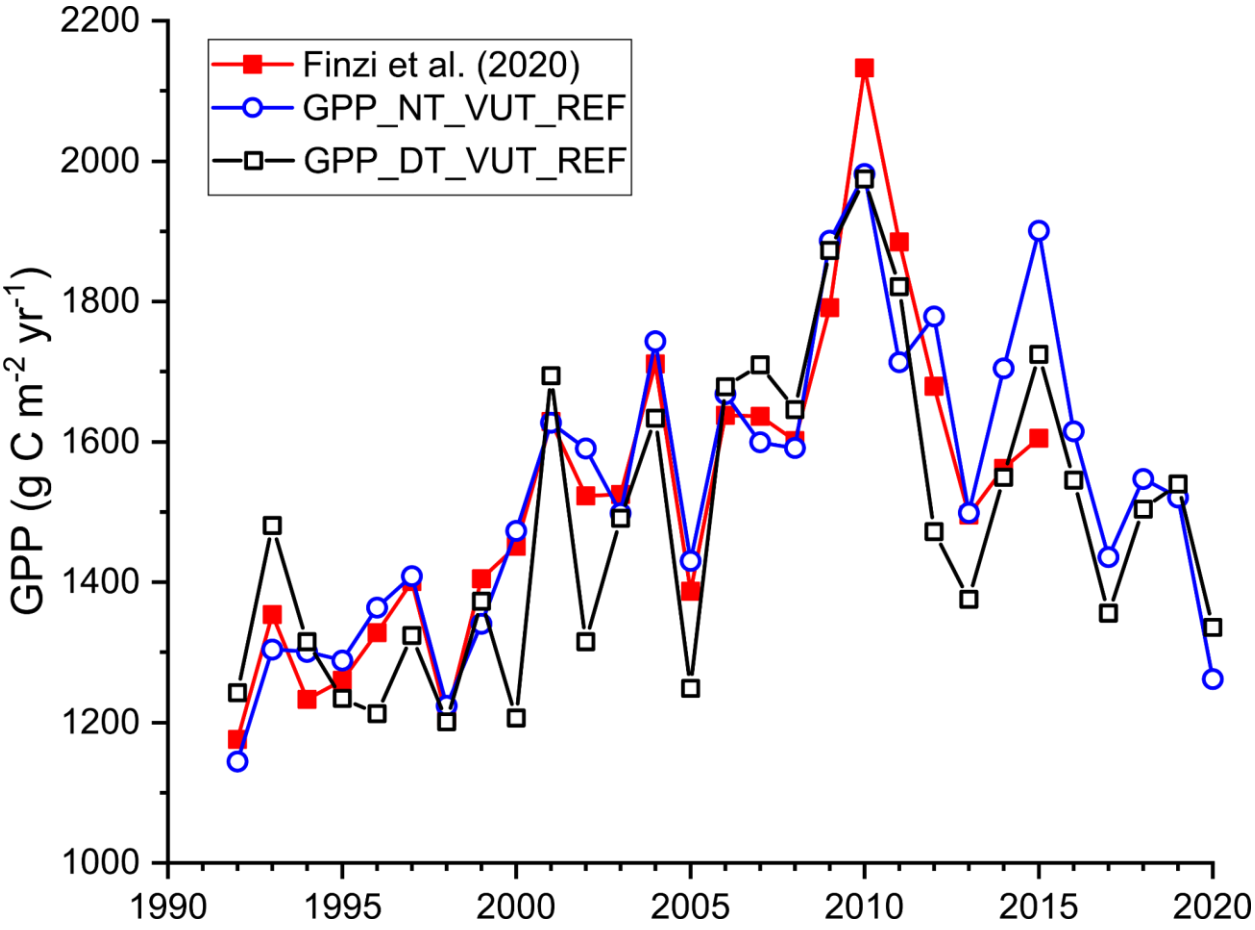

Supplementary Fig. 10. Estimates of annual gross primary production (GPP) at the AmeriFlux US-Ha1 (Harvard Forest) flux tower. Data are from Finzi et al. (2020) (ref. 19) for 1992–2015 and the AmeriFlux (Munger, 2022) database (ref. 56) for 1992–2020 using the GPP_NT_VUT_REF and GPP_DT_VUT_REF products. The two products differ in nighttime (NT) and daytime (DT) partitioning of net ecosystem exchange to obtain GPP. The GPP_NT_VUT_REF product compares favorably with the Finzi et al. data.

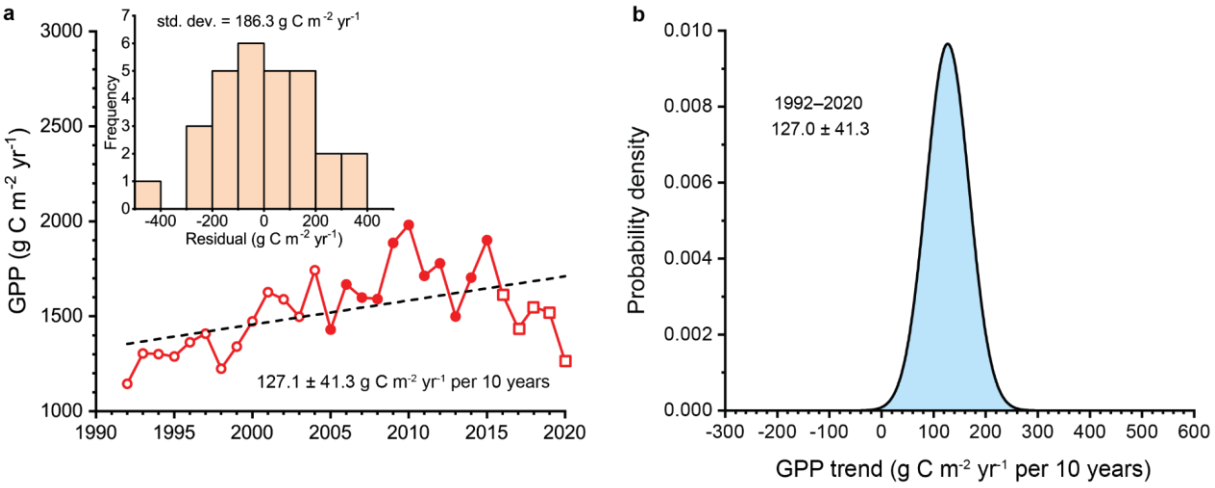

Supplementary Fig. 11. Statistical distribution of annual GPP trends sampled in Monte Carlo simulations using the AmeriFlux US-Ha1 (Harvard Forest) observations. (**a**) The full 1992–2020 AmeriFlux time series (ref. 56). Shown is the linear regression (dashed line) with the estimated slope ± standard error. Open circles show the years 1992–2004, closed circles extend the dataset to 2015, and open squares are the additional data to 2020. The inset panel shows the frequency distribution of the residuals. (**b**) Distribution of trends obtained with Monte Carlo methods in which annual GPP for each year from 1992 to 2020 is calculated as a random deviate about the regression line drawn from the distribution of residuals. The trend for the 29-year randomly sampled time series is estimated by linear regression, and the procedure is repeated 100,000 times to obtain the statistical distribution of the trend. The randomly sampled trends are normally distributed with a mean of 127.0 g C m^{-2} yr^{-1} per 10 years and a standard deviation of 41.3.